

OBSERVATIONS OF THE MAGNETIC FIELD AND PLASMA FLOW
IN JUPITER'S MAGNETOSHEATH

R. P. Lepping, L. F. Burlaga and L. W. Klein
Laboratory for Extraterrestrial Physics, Planetary Magnetospheres Branch
NASA/Goddard Space Flight Center, Greenbelt, Maryland 20771

J. M. Jessen and C. C. Goodrich
Center for Space Research, Massachusetts Institute of Technology, Cambridge, Massachusetts 02139

ABSTRACT. Large scale (many minutes to 10 hours) magnetic field structures consisting predominantly of nearly north-south field directions have been discovered in Jupiter's magnetosheath from the data of Voyagers 1 and 2 and Pioneer 10 during their outbound encounter trajectories. The Voyager 2 data, and those of Voyager 1 to a lesser extent, show evidence of a quasi-period of 10 hours (and occasionally 5 hours) for these structures. For all three spacecraft the changes in the field throughout these structures for many tens of hours are approximately restricted to a plane parallel to Jupiter's local magnetopause, according to a variance analysis of the field. Similar directional changes in the field occurred in the inbound magnetosheath for the Voyager spacecraft, but the occurrence was much less frequent, no quasiperiodicity was apparent, and the scale lengths were on average much shorter. The north-south components of the field and plasma velocity are strongly correlated in the outbound magnetosheath as observed by Voyagers 1 and 2, and the components orthogonal to the north-south direction show weak correlations. For both Voyager encounters the sense (positive or negative) of the north-south correlations has been directly related to the direction of the ecliptic plane component of the interplanetary magnetic field (IMF) using the field and plasma measurements of the non-encountering spacecraft. Some outbound magnetopause and bow shock crossings, on Voyager 2 especially, are phase locked in system III with some of the large scale magnetosheath field and plasma structures. These structures may be accounted for in terms of field line draping around the magnetopause of the convected IMF and solar wind, where the temporal properties are controlled by the motion and shape of a flattened magnetosphere which, in turn, depend on the rapid rotation of the current sheet within the magnetosphere.

Introduction

In situ measurements of the magnetic field and plasma near Jupiter by Pioneer 10 and 11 [Smith et al., 1976; Goertz, 1976; Kennel and Coroniti, 1977] and by Voyager 1 and 2 [Ness et al., 1979a, b; Bridge et al., 1979a,b; Siscoe et al., 1980] have demonstrated the existence of a bow shock (BS), a magnetosheath (MS), and a magnetosphere. All of these observations indicate the presence of a well-defined magnetopause on the dayside, similar to that of the earth. Krimigis et al. [1979] suggest that corotating magnetospheric plasma extends to the MS on the dayside; they infer that on the nightside there is a transition

from corotating plasma to a 'magnetospheric wind', but they report that the relation between this boundary and the magnetopause (MP) is not clear. Other observers have reported a clearly defined MP on the nightside. The stand-off distance of the Jovian MP is greater and more variable than was predicted by a model in which the momentum flux of the solar wind is balanced by the pressure of the planetary magnetic field. This suggests that at Jupiter (in contrast to earth) hot magnetospheric plasmas, particularly in the Jovian current sheet, play a significant role in balancing the momentum flux of the solar wind.

Little has been written about the magnetic fields and plasmas in the Jovian MS. In analogy with the earth's MS and on the basis of fluid calculations such as those of Spreiter et al. [1968], one might expect that, for an interplanetary magnetic field lying mainly in the ecliptic plane, the magnetic field in the MS would tend to be also in the ecliptic plane with random fluctuations about that plane. However, Lepping et al. [1981] found that the magnetic field in the Jovian MS tends to be either nearly north or nearly south (i.e., either parallel or antiparallel, respectively, with respect to Jupiter's rotation axis) for intervals ranging occasionally from many minutes to 10 hours, and the transitions from north (south) to south (north) tend to occur at 5 or 10 hour intervals. The north-south fields were observed both inbound and outbound, but they were observed most clearly outbound and close to the MP. The 5 and 10 hour changes were observed only on the outbound (tailward) passages of Voyagers 1 and 2, possibly because of the longer observing time there.

Highly inclined MS fields are observed occasionally in the earth's MS and to our knowledge there has been no report of analogous 12 and 24 hour changes. Thus, the Voyager data have revealed a new MS phenomenon, which seems to be a characteristic of the Jovian system.

The purpose of this paper is to present a comprehensive description of the Jovian MS magnetic fields and to speculate briefly on possible causes of these phenomena. We emphasize our Voyager 1 and 2 magnetic field observations and their relations to the plasma observations, but we also show that the same phenomena are present in the Pioneer 10 magnetic field data.

Spacecraft Trajectories and Model Boundaries

Figure 1 shows the trajectories of Pioneer 10 and the two Voyagers in Jupiter orbital coordinates as well as model boundaries of Jupiter's MP and BS, in the orbital plane, as estimated separately from the two Voyager en-

Copyright 1981 by the American Geophysical Union.

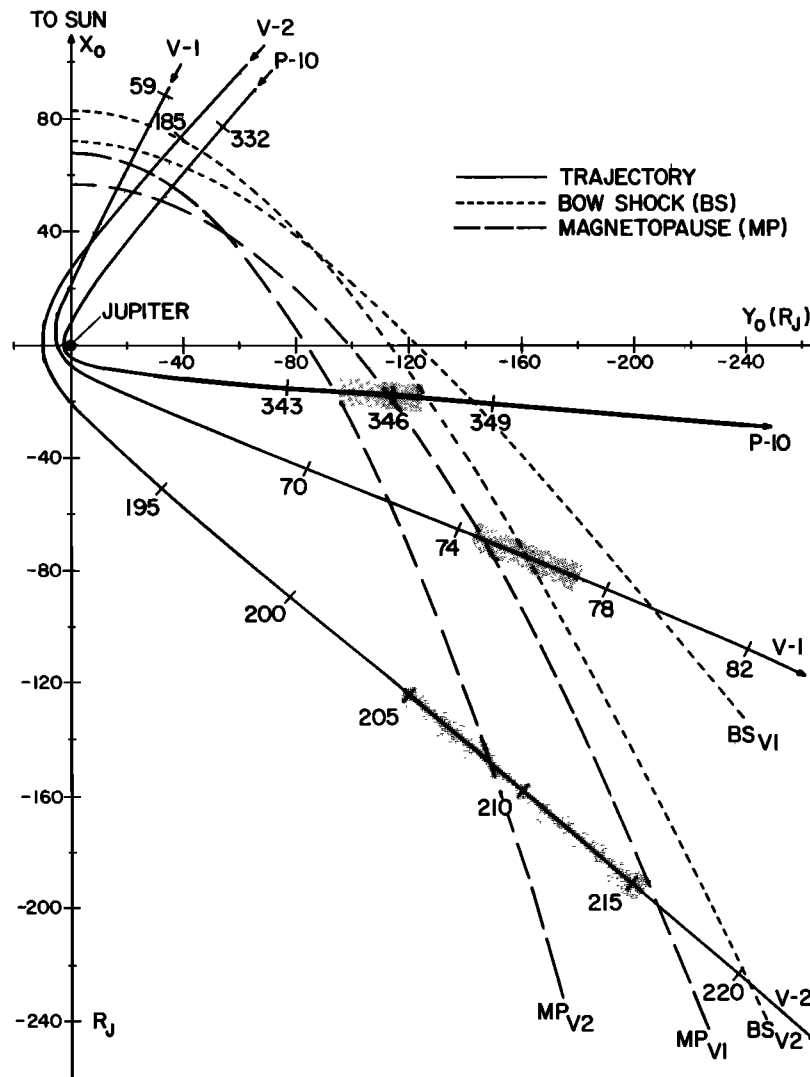


Fig. 1. The trajectories of Voyagers 1 and 2 (V-1, V-2) and Pioneer 10 (P-10) in the plane of Jupiter's orbit. Also shown are model magnetopause (MP) and bow shock (BS) boundaries [see Lepping et al., 1980] delimiting the average magnetosheath regions as observed by V-1 and V-2. The gray shaded regions along the trajectories are the 'early' magnetosheath bounded by the first outbound MP and first outbound BS. Day-of-year is given along the trajectories for various positions.

counters [see Ness et al., 1979a,b; Lepping et al., 1981]. The MP boundaries were modeled by fitting parabolas to the average inbound and outbound MP crossing points with the assumption of zero aberration due to planetary motion; such aberration at Jupiter is obviously small in comparison with solar wind direction changes over the three or four week period of encounter. The BS's were similarly modeled, except hyperbolas were used with the added constraint that estimated normals to the actual boundaries at the crossing points (based on averages) must agree with the models. The MP and BS model boundaries are meant to be only approximately representative, since the time scale for major changes in the solar wind is much shorter than the period separating the inbound and outbound series of crossings, for either spacecraft. Since the primary concern here is the outbound MS, also shown in Figure 1 are shaded regions denoting for

each spacecraft the region between the first actual outbound MP encounter and the first actual outbound BS encounter, i.e., the region where the MS closest to the MP was observed for each trajectory. These regions will be referred to as 'early magnetosheath.' Magnetosheath beyond this in time will be referred to as 'late magnetosheath.' A list of the MP and BS boundaries is given for Pioneer 10 by Intriligator and Wolfe [1976] and for the Voyagers by Bridge et al. [1979a, b] and Lepping et al. [1981].

The length of the shaded regions in the figure indicate how the width of the observed early MS increased dramatically from the Pioneer 10 outbound longitude (φ 0525 LT) to Voyager 1 (φ 0420 LT), and finally to Voyager 2 (φ 0300 LT). The lengths of these three regions were 30, 41, and 111 R_J ($R_J = 71,372$ km is Jupiter's radius), respectively. Since the outbound MS data are most extensive for Voyager 2, it is probably for

this reason that the MS effects studied are most prevalent in the Voyager 2 data.

Magnetic Field Observations Outbound

The magnetometers onboard the Voyagers have been described by Behannon et al. [1977]. For all of the magnetic field data discussed here the instruments were in the most sensitive range ± 8 nT, and quantized to a resolution of ± 0.004 nT per component. Absolute accuracy is estimated to be ± 0.09 nT per component, and the sample rate was 16.6 vectors/s throughout the periods of interest, but only 48 s averages were used for analysis and display in this study.

Figure 2 shows Voyager 1 48s average magnetic field data in heliographic (HG) coordinates for the two days 75 (= 16 March) and 76, 1979, which occur in the early MS. (A similar 2-day example of Voyager 2 early MS is given by Lepping et al. [1981].) Much of the scatter in λ in the figure is simply due to the extreme northward or southward inclinations of the field throughout this period. These data are reasonably typical of the early outbound MS of all three spacecraft, in that great variability in magnitude and direction is observed, most of the directional change is in latitude, and the field is predominantly in the northward or southward directions. From λ 0200 UT of 75 to λ 2200 UT, 76 (λ 44 hours) there are four major features in $\delta(t)$ separated approximately by the times: 1300 UT of 75, and 0100 UT and 1100 UT of 76. These major features are then λ 11 hours in duration on average. The extreme northward and southward directions of the outbound MS field as observed by Voyagers 1 and 2 is generally in mark contrast to the directions of the magnetotail field, which lies predominantly in or near the Jupiter orbital plane; see, for example, Figure 3 of Behannon et al. [this issue], which shows this regional comparison dramatically in vector form. However, as will be shown below, there is occasionally a significant southward component of the magnetosphere field

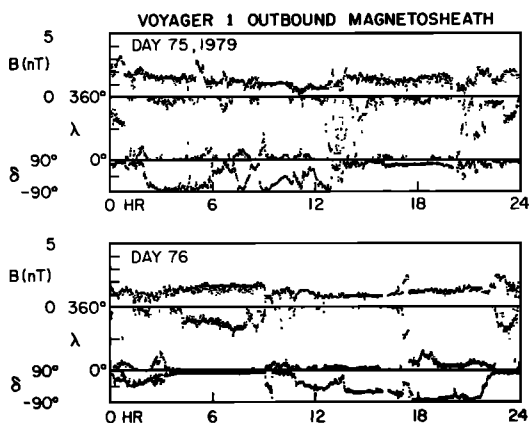


Fig. 2. A two-day example of 48-s averages of the magnetic field in the outbound MS as seen by Voyager 1. B is the magnitude of the field, λ is its longitude measured in a plane parallel to the sun's equatorial plane where $\lambda = 0^\circ$ is anti-sunward, and $\delta = 90^\circ$ is 'northward.' These angles are related to the heliographic R-T-N coordinate system by the following $B_R = B \cos\delta \cos\lambda$, $B_T = B \cos\delta \sin\lambda$, and $B_N = B \sin\delta$.

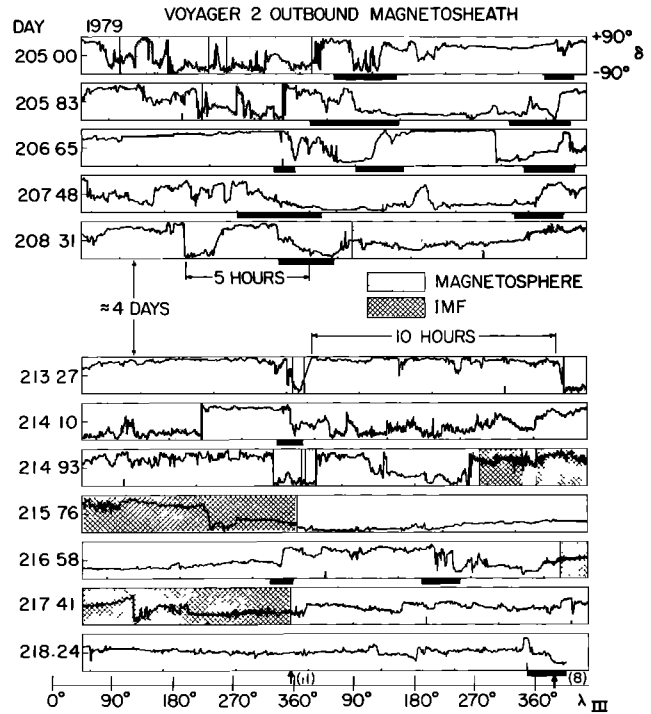


Fig. 3. The latitude (δ) of the magnetic field in the outbound MS along the Voyager 2 trajectory for a total of 12 Jupiter rotation periods; the central four days consisted primarily of magnetosphere data. Other segments of magnetosphere or interplanetary magnetic field (IMF) are designated by the shaded regions. The data is plotted with respect to Jupiter's system III longitude of 1965.0 (λ_{III}), and by day count; major tic marks denote starts of days. The horizontal black bars represent specific analysis intervals (see text).

also, especially as the MP is approached and in weak field regions such as the magnetotail current sheets.

For a broader view of the MS phenomenon, Figure 3 shows the latitude of the field for the Voyager 2 outbound MS for approximately ten days; regions of magnetosphere and interplanetary magnetic field (IMF) are denoted, and the 4-day separation is a continuation of magnetosphere data. The data are plotted with respect to System III (1965) longitude of the sub-spacecraft position, with two 360° cycles (plus 45° overlap) per panel, as well as by calendar day. Major tic marks on the time axis denote start-of-day, and one hour of data is repeated at the start of each panel in order that features are not lost at $\lambda_{III} = 45^\circ$. Again latitude variations occur throughout the entire ten days and are especially dramatic during the early MS, which ends (by definition) at the first outbound BS at 1441 UT on 215. Various λ 5 and λ 10 hour features appear throughout, and two of these are identified. The Voyager 2 data, in fact, demonstrate this large scale 5 and 10 hour latitude variation more clearly than the Voyager 1 data.

It is evident from Figure 3 that prominent 'events' were most probable at $\lambda_{III} \approx 360^\circ$ (see vertical arrows at bottom). By an 'event' we mean any one of the four occurrences: (1) a major north-south change of δ , (2) a major south-north

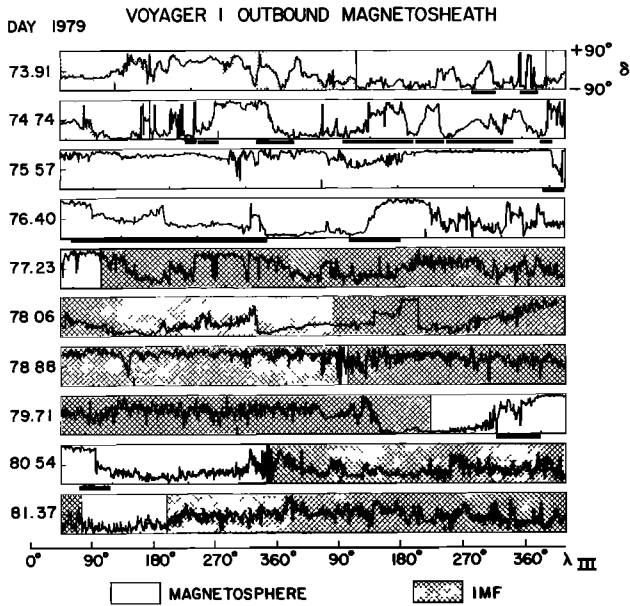


Fig. 4. The latitude (δ) of the magnetic field in the outbound MS along the Voyager 1 trajectory. See caption of Figure 3.

change of δ , (3) MP crossing, or (4) BS crossing. Eleven such events occur for the first arrow, and eight for the second arrow. This suggests a synchronization of field latitude changes and MP and BS motions jointly with the planetary rotation period (9.92492 hours for System III, 1965). The case for such events occurring with a ~ 5 hour period is much weaker, but 5-hour features in $\delta(t)$ are present. Note that there is much less variability in $\delta(t)$ in the 'late' MS.

As was mentioned above for Voyager 1 there was considerably less outbound early MS data; nevertheless, some of the same characteristics of the Voyager 2 MS are seen in a comprehensive view of

Voyager 1 data. Figure 4 similarly shows the latitude of the Voyager 2 field as a function of system III position of the spacecraft for ~ 8 days, ~ 3.5 days of which are MS data. The obvious similarity is in the distribution of δ itself, but the 5 and 10 hour structures are barely discernible if at all, as mentioned above (Figure 2 and associated text). Some of the complexity of structure may be due to the unusually variable IMF as evidenced in the latter half of the figure. There is a weak synchronization of events; for example, at $\lambda_{III} = 90^\circ \pm 20^\circ$ there are four BS crossings, one MP crossing, two major north-south MS δ changes, one major south-north δ change, and a minor north-south change. There are other weaker, synchronized events. To draw a broader comparison of features in the MS and of its boundaries, we proceed further upstream to the position of Pioneer 10.

Figure 5 shows the latitude (in an S-J coordinate system--see Smith et al. [1976] for a description) of 1-min averages of the magnetic field as a function of time for seven days, approximately 3-1/2 days of which are MS data. Again 'northward' and 'southward' magnetic fields are evident, there is a weak suggestion of a 10-hour structure (e.g., 0350 UT to 1310 UT on 345^d), and the BS crossings on 346^d are separated almost exactly by 5 hours (1453 UT and 1951 UT) as identified by Intriligator and Wolfe [1976]. And very nearly 5 hours prior to the first outbound BS, a pair of MP crossings occur (at 0943 UT and 0958 UT on 346^d). By 349^d the latitude angle of \vec{B} approaches lower values, as it did in the late MS of Voyager 2.

Magnetic Field Analyses

A qualitative examination of the outbound Voyager MS field data indicates that the large scale directional changes (over many minutes to 5 hours) occur primarily in a plane whose normal is approximately parallel to the modeled MP normal

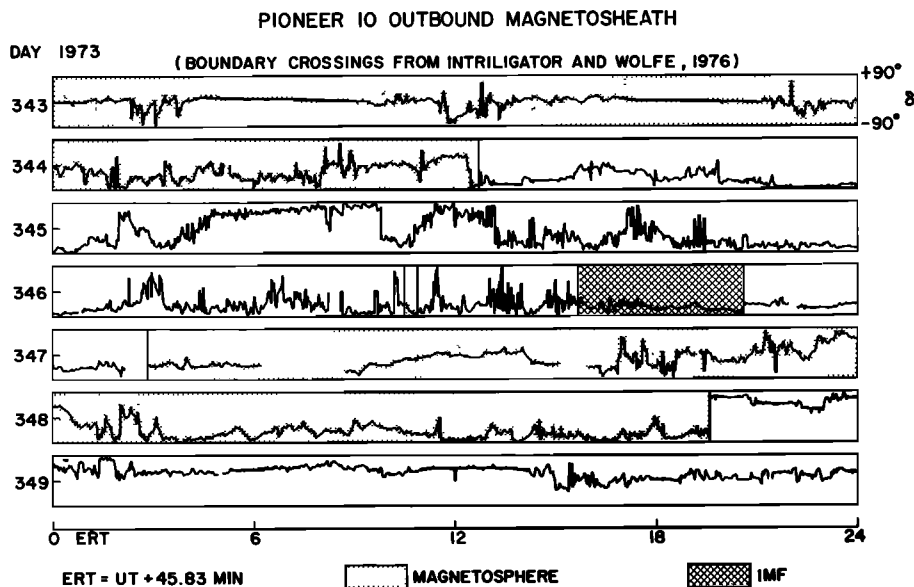


Fig. 5. The latitude (δ) of the magnetic field in the outbound MS along the Pioneer 10 trajectory. The display is similar to that of Figure 3 except δ is given as a function of earth receive time (ERT); its relationship to spacecraft UT is given at the bottom.

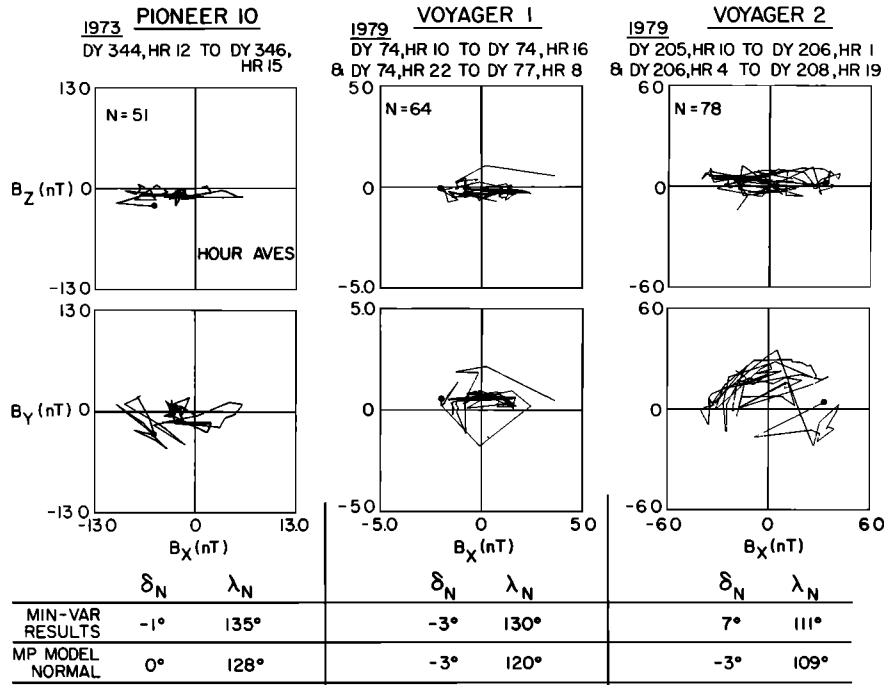


Fig. 6. Hodograms of the magnetic field for hour averages for Voyagers 1 and 2 and Pioneer 10 over time intervals listed at the top. N is the number of hour averages used. The plots are given in a variance coordinate system for each example (see text), where Z is in the minimum variance direction for each. The black dot denotes the starting time. The table at the bottom compares the MP model normal from Figure 1 with the minimum variance direction in heliographic coordinates (δ_N, λ_N).

(obtained from the fit to a parabola) for each encounter. In the HG coordinate system the MP model normals are $\lambda_{HG} = 120^\circ, \delta_{HG} = -3^\circ$ for Voyager 1 and $\lambda_{HG} = 109^\circ, \delta_{HG} = -3^\circ$ for Voyager 2 [see Lepping et al., 1981]. To demonstrate this quantitatively, a minimum variance analysis of the field according to the method of Sonnerup and Cahill [1967] was carried out using 78 one-hour averages of Voyager 2 data: 1000 UT of 205^d to 1900 UT of 208^d, excluding the three hours of magnetosphere data on 206^d (see Figure 3). Over the 78 hours the Voyager 2 trajectory covers an X_0 range of 22 R_J (see Figure 1), and over this range the model MP normal changes by only 0.9°. The resulting minimum variance direction was $\lambda_{HG}(2) = 111^\circ, \delta_{HG}(2) = 7^\circ$, which is in excellent agreement with the model normal. The ratio of intermediate to minimum eigenvalues (E2/E3) was 7.9, the ratio of maximum to intermediate eigenvalues (E1/E2) was 23.8, indicating that the estimated minimum variance direction is well determined; a value of E2/E3 below 2.0 indicates a poorly determined variance ellipsoid [Lepping and Behannon, 1980]. Also $|\langle B_z \rangle|/\langle B \rangle = 0.16$ and $\langle B \rangle = 3.0$ nT, where B_z is the component along the minimum variance direction, B is the magnitude of the field, and the braces $\langle \rangle$ indicate an average over the 78 hours.

Using 64 one-hour averages of Voyager 1 data over the MS period 1000 UT of 74^d to 0800 UT of 77^d, and excluding six hours of magnetosphere data on late 74^d (see Figure 4), the following minimum variance results were similarly obtained: $\lambda_{HG}(1) = 130^\circ, \delta_{HG}(1) = -3^\circ$; E2/E3 = 3.2; E1/E2 = 16.0; $|\langle B_z \rangle|/\langle B \rangle = 0.23$; and $\langle B \rangle = 1.4$ nT. Again the minimum variance direction is in good agree-

ment with the Voyager 1 model MP direction, differing by only $\sim 10^\circ$ and it is reasonably well determined according to the eigenvalue ratios. Over the 64 hours the Voyager 1 trajectory covers an X_0 range of 15 R_J , and over this range the model MP normal changes by only 1.3°.

Notice that the average outbound MS field $\langle B \rangle$ was approximately twice as strong for Voyager 2 as for Voyager 1. Also $|\langle B_z \rangle|/\langle B \rangle$ was a little smaller for Voyager 2, although in both cases its value indicates a relatively weak component of the field normal to the plane in which most of the variation is taking place, on average. Figure 6 (center and right panels) shows hodograms of the Voyager 1 and 2 hour averages in the coordinate system defined by the derived variance ellipsoid: Z is along the minimum variance direction, and X and Y are along the maximum and intermediate variance directions, respectively. Below the hodograms are the associated minimum variance normals and the MP model normals for comparison. An outstanding feature of the hodograms is the tendency of the field in the X-Y plane to form nested arcs for a large fraction of the analysis intervals, implying clear repetition. Also notice that both the variation of B_z and its mean are significantly smaller than $\langle B \rangle$ for both spacecraft. So the MS field at any 'instant' and its coherent, undulatory variations are fairly well contained in a plane whose normal is nearly parallel to the local MP normal for each data set.

The Pioneer 10 outbound MS was similarly analyzed by using one-hour averages of the magnetic field over the period 1200 UT of 344^d to 1500 UT of 346^d, 1973. The following variance results

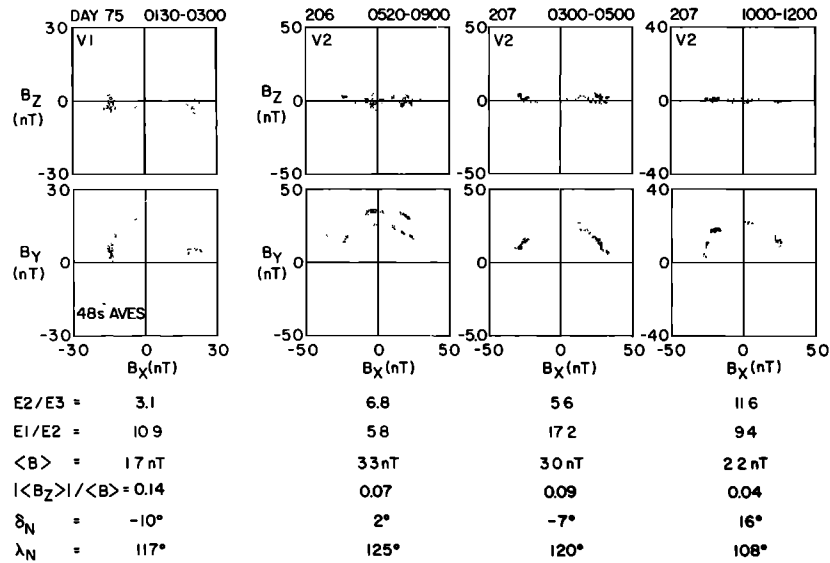


Fig. 7. The magnetic field (48-s averages) plotted in a variance coordinate system for each example (Z in minimum variance direction) for Voyager 1 (V-1) and Voyager 2 (V-2). These examples are from those denoted by black horizontal bars in Figures 3 and 4.

were obtained: $\lambda(10) = 135^\circ$, $\delta(10) = -10^\circ$; $E2/E3 = 8.3$; $E1/E2 = 4.2$; $| \langle B_z \rangle | / \langle B \rangle = 0.18$; and $\langle B \rangle = 4.3$ nT. The associated hodogram in the variance coordinate system is shown in Figure 6 (left panels). The minimum variance normal, which was well determined according to the eigenvalue ratios, and model normal (Voyager 1 model MP normal) differ by only 7° , and again the ratio $| \langle B_z \rangle | / \langle B \rangle$ is small and consistent with those for Voyagers 1 and 2. There is a pattern of repetition in the X-Y plane, but not in the form of an arc structure. Again the variation in B_z is small in comparison with $\langle B \rangle$, and interestingly $\langle B_z \rangle$ appears to increase in going from Pioneer 10 to Voyager 1 and again to Voyager 2, i.e., as we go tailward, as the upper panels of Figure 6 show.

Similar analyses were carried out for portions of most of the large features individually using Voyager 1 and 2 48s averages of the field. The specific analysis intervals are shown in Figures 3 and 4 as black horizontal bars beneath the regions of interest. There were 14 such intervals for Voyager 1 and 14 for Voyager 2. Figure 7 shows four examples of the 48-s average points plotted in the derived minimum variance coordinate system for each case, with their associated numerical results below. These were fairly characteristic of the overall 28 cases, excluding a few poor cases.

Notice that directions (δ_N, λ_N) parallel to the directions of minimum variance were close to the MP model normal directions and were well determined. Also it is striking that double arcs appear in the X-Y plane (i.e., intermediate-maximum variance plane) of the Voyager 2 data indicating that the field partially retraced its path more or less half way through its angular excursion. Notice that the points tend to cluster more at the ends of the arcs than in the centers. Even though they are not discontinuities in the usual sense, these large scale features more closely resemble tangential dis-

continuities than rotational discontinuities in that they have small ratios $| \langle B_z \rangle | / \langle B \rangle$, i.e., the field changes are well confined to a plane, which is parallel to the local MP in each case. This was true of almost all of the cases studied, and on average this ratio (0.17 for Voyager 1 and 0.29 for Voyager 2) was comparable to what it was for the analyses using hour averages over several days as discussed above.

Figure 8 summarizes the full set of minimum variance normals from the results of both spacecraft, and compares them with the MP model normals. With only a few exceptions the minimum variance normals cluster very closely around the model normals. Since the minimum variance normals usually were associated with a large ratio of the intermediate to minimum eigenvalues and since changes in the field perpendicular to these normals subtended large arcs, they were very well determined, having error cones of half-angle possibly in the neighborhood of a few degrees. Hence, the scatter shown in Figure 8 is probably real in the sense that it mainly represents an actual time-variation in the direction of the normal to the plane of maximum variance over the days representing the full sample sets. This is not surprising since bulk and wave motions of the MS and its boundaries are expected.

In order to obtain a statistical overview of the distribution of latitudes of the field in the outbound MS over as broad a range of Jovian longitude as possible, histograms of δ were generated by using 48-s averages for the early and late MS separately from the data of all three spacecraft. Also for comparison and for each spacecraft a histogram of δ was computed from the magnetosphere data just prior to the first outbound MP crossing combined with magnetosphere data between subsequent MP crossings. To complete the comparison similar histograms were computed for the IMF data by combining that data between BS crossings with a sample obtained after

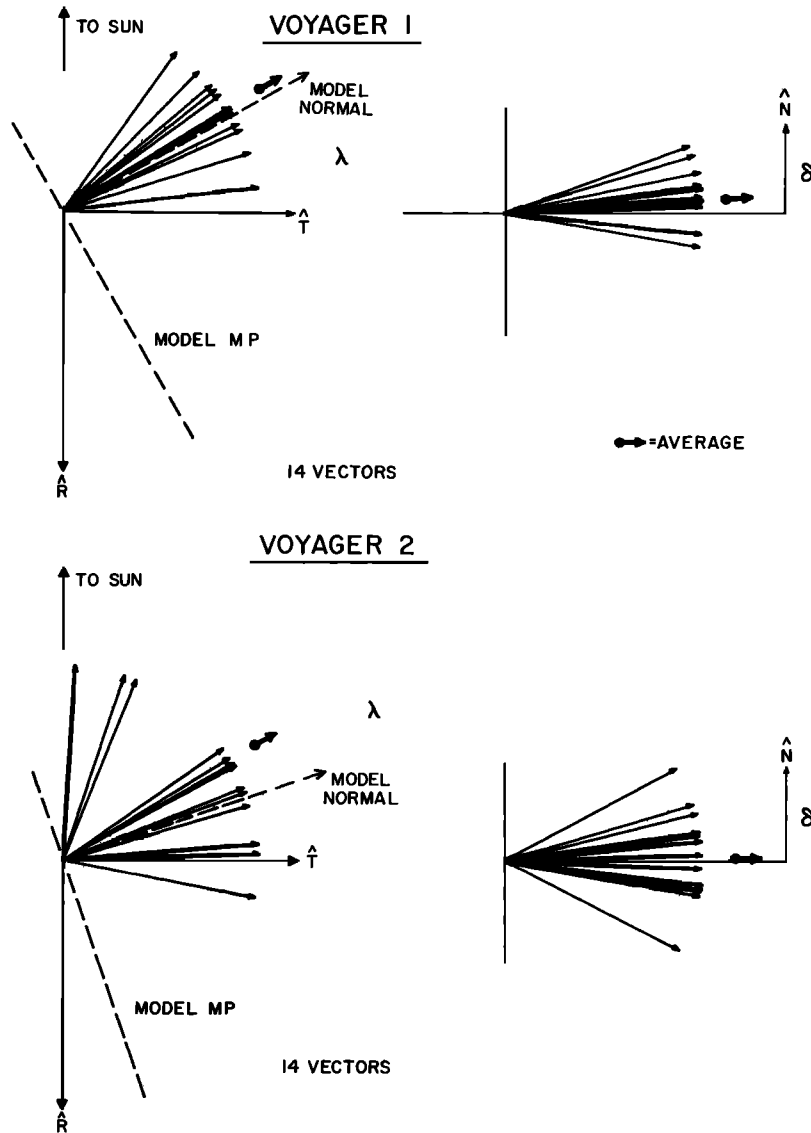


Fig. 8. Unit normals along the minimum variance direction for the 28 analysis intervals shown in Figures 3 and 4 as black horizontal bars in terms of the longitude λ and latitude δ . R, T, and N are defined in the caption of Figure 2. The short arrow represents an average of all normal estimates. The dashed line (and dashed arrow) represent the model MP (and its normal) for comparison.

the last BS crossing. The times for the Voyager MP and BS crossings are given by Lepping et al. [1981] and for Pioneer 10 by Intriligator and Wolfe [1976]. The resulting histograms are given in Figure 9. The magnetosphere histograms provide no surprises. They peak at $\delta \approx 0$ and show a considerable proportion of the distribution toward negative δ 's as expected for Jupiter's magnetosphere and tail [Smith et al., 1976; Ness et al., 1979b,c]. (See the top two panels of Figure 5 for an example of why the distribution of magnetosphere δ is disproportionately negative.) The early MS histograms have a bimodal appearance, as expected from fields that spend most of the time at high (+/-) latitudes as Figures 3, 4, and 5 have indicated. The reason for the lack of reproducibility from one spacecraft position to the next for the early MS data is at least partially due to the short periods of

time spent in the early MS by Pioneer 10 and Voyager 1, as measured in planetary rotation periods, which provides biased statistics. This is even more true for the late MS histograms; for example, notice that only 0.72 days of data could be used for Voyager 1 late MS. However, Pioneer 10 and Voyager 1 late MS distributions are similar, even if they are of opposite polarity with respect to polarity. This is in marked contrast to the Voyager 2 late MS, which is rather flat and peaks near the center (after some liberal smoothing). Apparently, the mechanism causing the large north-south structures diminished in effectiveness for Voyager 2 with respect to the previous encounters, either as a function of time or because Voyager 2 has travelled a greater distance from the MP's most probable position (supposedly the model position) than did the two earlier spacecraft or for some as yet unknown

δ - DISTRIBUTIONS (48 SEC AVERAGES)

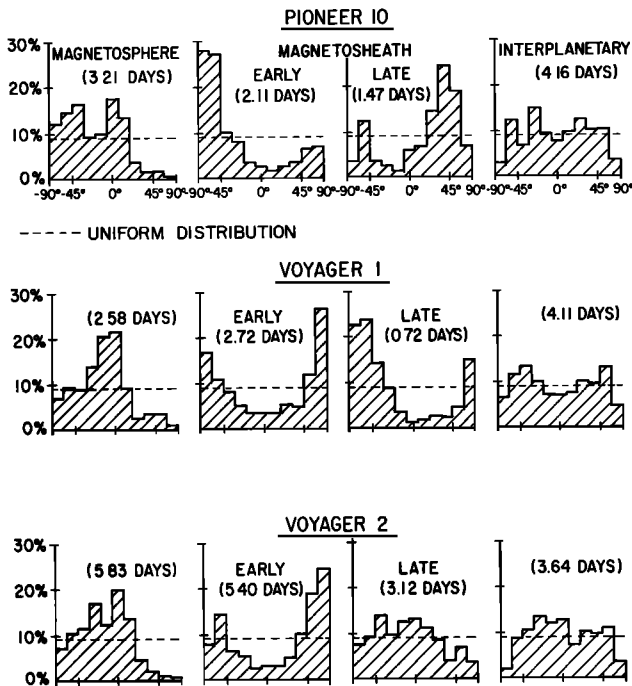


Fig. 9. Percent histograms of the latitude (δ) of the magnetic field (48-s averages) for Pioneer 10 and Voyagers 1 and 2. The latitude is strictly in heliographic coordinates (Figure 2 caption) for the Voyagers but is in the S-J system for Pioneer 10 [see Smith et al., 1976]; the difference is small and unimportant for our purposes here. The histograms are divided into four categories: the magnetosphere adjacent to the outbound MP, the early and late outbound MS defined in the text, and the IMF adjacent to the outbound BS. The number of days of data is given in parentheses for each histogram, and the histograms are plotted by $\frac{1}{2}$ equal solid angle buckets.

reason. The interplanetary distributions are considerably flatter than all of the others, but surprisingly they are not gaussian-like, as would be expected for most large IMF data samples. In any case, they do not portray the rather clear bimodal shape of most of the MS distributions.

In order to provide an example of the distribution of the latitudes (δ) of the IMF at the orbit of Jupiter, for comparison with those given in Figure 9, 480 Voyager 2 hour averages of the IMF upstream of Jupiter (163° to 183°, 1979, just before the first inbound BS) were used. Figure 10 displays the results along with distributions of B and λ for completeness. Notice that all three quantities have fairly standard distributions. Although the B distribution is somewhat broad, its mode is close to what is expected (0.5 nT) from the IMF model of Behannon [1978], and the peaks in λ are also where the model predicts $\lambda = 100^\circ$ and 280° , indicating a tight spiral field in the R-T plane. More importantly, the δ distribution is approximately gaussian peaking near zero. Use of the R-T-N system instead of the model system (ecliptic) causes an $\approx 3^\circ$ shift in latitude for a tightly wound field for this period. It is very interesting that this δ

distribution, being quite typical, is so markedly different from the post-Jupiter IMF distributions shown in Figure 9.

Correlation of Plasma Flow Velocity and Magnetic Field

In this section we describe a correlation that has been observed between the magnetic field and the ion-plasma flow velocity in the outbound Voyager MS. The Plasma Science Experiment (PLS) has been described by Bridge et al. [1977]. The proton energy range of the instrument is 10-5950 eV, and a full spectrum is sampled over a 96-s measurement cycle for the intervals of concern here. Figure 11 shows daily plots of the N-components of the plasma velocity (\vec{V}) and magnetic field (48-s averages) for days covering the earliest portion of the outbound MS for both Voyagers, where 'N' represents the component normal to the sun's equatorial plane, positive northward (see caption of Figure 2). The V_N and B_N scales are inverted with respect to each other for all panels, except for 205^d of Voyager 2, in order to show the correlation between V_N and B_N most clearly. There is a strong positive correlation on 205^d and an equally remarkable negative correlation for the other days (with the exception of the brief positive correlation early on 206^d). In fact, for all of the remaining outbound MS data of both spacecraft (i.e., for all those not shown in this figure) a pointwise negative correlation between V_N and B_N is observed (there are significant but much weaker correlations in the components of \vec{V} and \vec{B} orthogonal to \hat{N} throughout the outbound MS also). The IMF and the solar wind velocity in the proximity of the outbound BS's were examined in light of this MS phenomena, and such correlations were not found, although non-Alfvénic compressional fluctuations were observed. Briefly summarizing: a negative correlation in V_N versus B_N occurred for all of the outbound Voyager 1 and Voyager 2 MS, except for a positive correlation in the very earliest Voyager 2 interval, ending somewhere between 0051 and 0409 UT of 206^d, during which the spacecraft 'returned' to the magnetosphere.

PRE JUPITER ENCOUNTER - IMF (5.24 AU)
VOYAGER 2, 1979, DAYS 163 TO 182

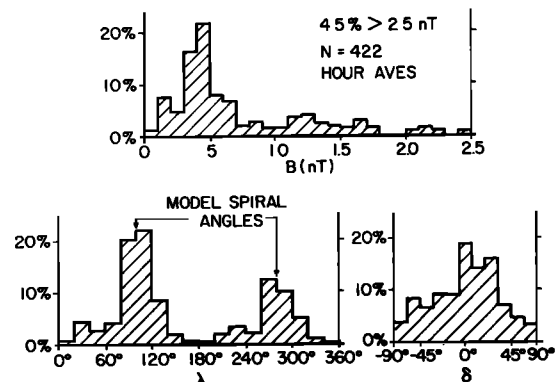


Fig. 10. An example of Voyager 2 IMF statistics in the form of distributions of B, λ , δ (hour averages) over 20 days at $r = 5.2$ AU, i.e., just prior to the first Voyager 2 BS encounter, for comparison of the IMF histograms of Figure 9.

The MS magnetic field is a modification of a former IMF that has been convected past a turbulence-producing BS and distorted by the MS flow field in which it is embedded; this, in turn, depends on the shape and motion of the obstacle to flow, Jupiter's magnetosphere in this case. If magnetic merging occurs at the MP for instance, the resulting MS field would experience further alteration. Hence, any hope of understanding the newly discovered V_N-B_N MS relationship requires knowledge of at least the upstream IMF. In order to determine the IMF just upstream of Jupiter, we used the known plasma and field quantities measured by the nonencountering spacecraft and projected hour averages of these quantities temporally forward in the case of the Voyager 1 encounter and backward for the Voyager 2 encounter. This prediction method assumes constant radial expansion velocity for the solar wind and neglects evolution; this usually succeeds well for intervals devoid of interplanetary shocks, which was the case for the intervals of interest here.

The predictions indicate that for the V_N-B_N negative correlation periods of both encountering spacecraft the IMF at Jupiter had a consistent and significant positive B_T component (see caption of Figure 2 for the definition), i.e., $\lambda_{IMF} \sim 60^\circ-90^\circ$. And for the period when V_N and B_N were positively correlated (Voyager 2, late 204^d throughout, 0051 UT of 206^d) the IMF at Jupiter had a consistent and significant negative B_T component, i.e., $\lambda_{IMF} \sim 270^\circ$. In particular, an IMF sector change as observed at Voyager 1 was predicted to occur at the nose of Jupiter's MP at about 2000 UT \pm 8 hours on 204^d. It was then estimated to arrive at Voyager 2 in the downstream MS at 1700 UT \pm 10 hours on 205^d, after traversing \sim 300 R_J at an average speed of \sim 290 km/s along the curved MP. This is consistent with the alteration from positive to negative V_N-B_N correlation occurring at \sim 0200 UT \pm 2

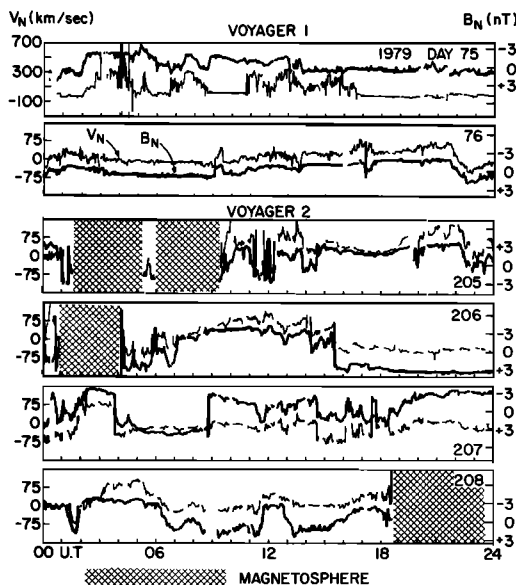


Fig. 11. Daily plots of the N-components of the plasma velocity V and magnetic field B in the outbound MS for Voyager 1 (2 days) and Voyager 2 (4 days). The heavy curves are B_N , and the cross hatched regions denote the magnetosphere.

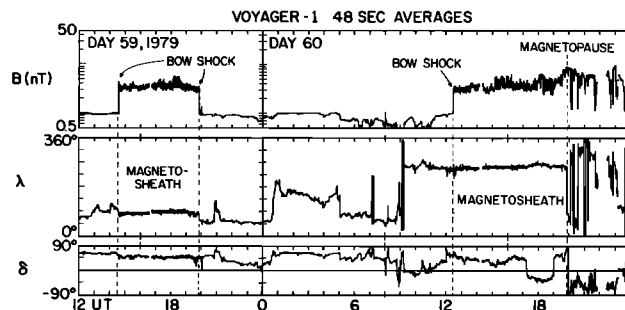


Fig. 12. An example of Voyager 1 magnetic field data (48-s averages) around the time of inbound multiple BS crossings which compares MS data near the MP to that closer to the BS.

hours on 206^d. The estimated average MS speed of 290 km/s used above was based on the Spreiter et al. [1968] steady state model of MS flow for the earth's case, a projected solar wind speed of \sim 400 km/s based on the Voyager 1 data, and the preliminary assumption of zero signal propagation speed with respect to the bulk MS flow. (The actual speed of signal propagation is small in comparison with 290 km/s, so it can be neglected for our purposes here; this will be further developed in the discussion).

It was also interesting to note that neither the positive nor negative correlation periods possessed any obvious relationship to the projected IMF B_N component (i.e., to δ_{IMF}). Before leaving Figure 11 it should be remarked that in this component format (as opposed to the δ -angle format) various 5 and 10 hour features again appear, even in the Voyager 1 data, which was less clear in Figure 4, for example. Also notice the \sim 5 hour V_N structure on Voyager 1, 75^d, between \sim 1100 and \sim 1630 UT, a period when V_N-B_N are only weakly correlated, and on late 205^d for \sim 10 hours where V_N and B_N are strongly correlated.

The solar wind and the IMF for the periods shown in Figures 3 and 4 and for brief periods beyond the last outbound BS's were visually surveyed for possible correlations similar to those in the MS, but no obvious correlations were found, but again compressional waves were observed (at least on Voyager 1).

Magnetic Field Observations Inbound

An examination of the inbound MS data of both Voyager spacecraft reveals magnetic field features that in some respects resemble those of the outbound MS. As an example, Figure 12 shows Voyager 1 field data for 59^d and 60^d, i.e., around the time of multiple BS crossings pre-Jupiter encounter (see Figure 1). Notice that the MS between 1434 and 1954 UT of 59^d is fairly steady on a scale of tens of minutes and deviates little in direction from the upstream IMF, even though highly inclined. In contrast to this steady MS field close to the BS and far from the MP, the MS occurring between 1227 and 1956 UT of 60^d shows both positive and negative inclinations especially as the MP is approached. This is not an uncommon feature of inbound Voyager MS fields which are apparently close to the MP. However, there does not seem to be a case for 5 and 10 hour variations for any of the inbound MS data

from Voyager 1 or 2. This is possibly due to the fact that most inbound MS intervals are too short, because of the nature of the spacecraft trajectory, for such long period phenomenon to be properly identified. Alternately, perhaps such repetitiveness either does not occur in the inbound MS or is a subtle effect there.

A preliminary variance analysis of several of the highly inclined magnetic field structures in the inbound MS of Voyager 1 and 2 [Lepping et al., 1981] indicates that the minimum variance normals are approximately parallel to the local MP model normal, just as was found for the outbound MS structures.

Discussion and Preliminary Interpretation

All of the observations discussed above have referred to the 'dawnside' MP, MS, and BS. One might ask if the dawn and dusk MS regions are similar with regard to the various features discussed in light of a possible asymmetry brought about by Jupiter's rapid rotation: anti-parallel plasma streams at the dawn MP (i.e., corotating magnetospheric plasma moving \sim sunward versus \sim tailward moving MS flow) and presumably parallel streams at the dusk MP, in Jupiter's orbital plane. The answer must wait for future observations, but it would be surprising if there were no marked average differences.

Related to this question of asymmetry is the question of possible magnetic field line merging [Vasyliunas, 1975] at the dawn versus dusk MP's. It appears that such merging would be more probable at the dawnside, if possible at the MP generally, because of the anti-parallel streaming, the highly to moderately probable southward magnetosphere field (see Figure 9), the highly likely (\sim 0.5 probability) condition that B_N will be northward in the MS (Figure 9), and the known dynamic state of the dawn MP which probably consists of bulk and wave motions as in the case of the earth's MP. Probably all of these conditions hold for the duskside MP as well, with the important exception of the anti-parallel streaming. At the dawnside MP then, we envision frequent occasions when parcels of plasma with embedded fields of oppositely directed and significant B_N components are moving directly toward each other with relative speeds of up to $\sim 10^3$ km/s. That these conditions cause magnetic merging at Jupiter has not been proven, so we will discuss it no further here; however, it is a possibility that will be investigated further. In any case, it is probably not necessary to invoke merging to explain the outbound MS phenomena, as we attempt to show below.

We now discuss the overall aspects of the observations that have been presented and consider the following questions: (1) what causes the north/south field orientations and changes that occur in a plane parallel to the local MP, (2) what is the cause of the 5 and 10 hour structure, (3) why are V_N and B_N so strongly correlated, (4) why are these features occasionally synchronized with MP and BS crossings, and (5) is there an analogous, but yet unidentified, phenomenon in the earth's MS?

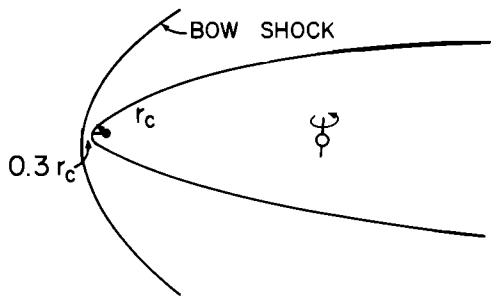
We believe that the first three questions might be explained in terms of the draping of MS fields around a flattened and dynamic Jovian magnetosphere, i.e., flattened approximately

along the direction of the planetary rotation axis. First consider the shape of the magnetosphere. Studies based on Pioneer data and theoretical considerations suggest that Jupiter's magnetosphere is significantly smaller in its north-south direction (Z_E) than in its east-west direction (Y_E) in the $X_E = 0$ plane, for instance [e.g., see Hill et al., 1974; Beard and Jackson, 1976; and Engle and Beard, 1980]; Z_E is parallel to the rotation axis of Jupiter and X_E is sunward, and the subscript E refers to the equatorial coordinate system. The model developed by Connerney et al. [this issue] which includes the effects of the inner current sheet and which is based on a fit to Voyager 1 and 2 magnetic field data supports this idea. Engle and Beard [1980] estimate that $Z_E/Y_E \sim 0.6$, where Y_E and Z_E are measured in the $X_E = 0$ plane. It was suggested to us (A. Dessler, private communication, 1980) that there is an independent means of testing the idea that Jupiter's magnetosphere is significantly flattened (approximately along planetary rotation axis) by applying aerodynamic theory [see, for example, Krasnov, 1970] and comparing the ratio $\Delta R/R_{Sp}$ for Jupiter and earth, where R_{Sp} is the solar wind stagnation distance (Jovicentric), $\Delta R = R_{BS} - R_{Sp}$ and R_{BS} is the subsolar bow shock distance. For a fixed Mach number, as the obstacle to supersonic flow becomes more sharp-nosed (represented by Figure 13a) in contrast to a moderately offset sphere with a much larger front-side radius of curvature (r) (Figure 13b, representing the earth's front-side magnetosphere), the ratio $\Delta R/R_{Sp}$ approaches zero. This ratio is 0.26 and 0.22 for the Voyager 1 and 2 encounters, respectively, and is 0.33 for earth on average [Fairfield, 1971]; the Voyager estimates are based on model BS and MP boundaries [Lepping et al., 1981]. Since the Pioneer and Voyager observations clearly reveal an approximately parabolic shape for the MP (on the dawnside at least) in the $X_0 - Y_0$ plane (Figure 1) whose characteristics are such that $X_0 < Y_0$, then it is likely that in the $X_0 - Z_0$ plane $X_0 > Z_0$, and the magnetosphere is significantly flattened along the Z_0 axis (notice that the Jupiter equatorial coordinates and orbital coordinates are aligned to within about one degree). Concerning the large scale dynamic behavior of the tailward portion of the magnetosphere, Behannon et al. [this issue] show that observations of Jupiter's magnetotail strongly suggest that the predominant motion is one of rocking of the tail about the planet-sun axis (X_E axis in Figure 14). Their arguments are based on analyses of the orientation of the tail current sheet as seen by Voyager 2, as well as on modeling of the gross tail motion determined by current sheet crossing times from Voyagers 1 and 2. Thus, we envision a large, flattened magnetosphere of Jupiter rocking primarily about the planet-sun line with an \sim 10-hour period. However, other motions of the magnetodisc probably cannot be ignored [e.g., see Carbary, 1980; Behannon et al., this issue], especially the precession of the disc about the rotation axis close to the planet ($\lesssim 25 R_J$). Also our picture of a 'flattened' magnetosphere is not meant to exclude such similar geometrical shapes as an earthlike magnetosphere with a bulge running around its equatorial region, for example.

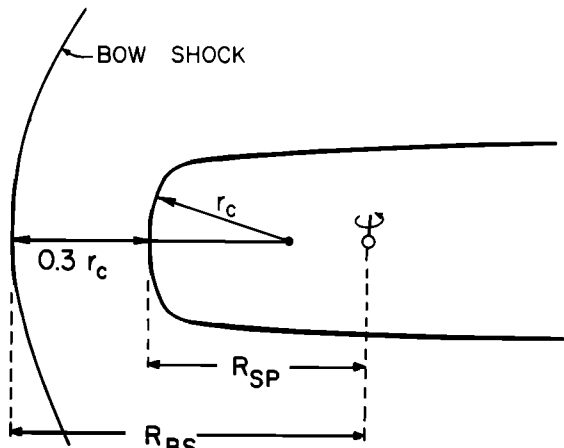
Let us consider a kinematic model for the rocking motion of a flattened magnetosphere. We define β to be the angle between the rotation axis (\hat{Z}_E) and the projection onto the Y_E-Z_E plane of the normal (\hat{N}) of the planet's dipole direction, (\hat{N}) to the inner magnetosphere current sheet; see Figure 14. In 9.925 hours β will complete a full oscillation, but in 4.962 hours it completes a minimum to maximum excursion: $-9.6^\circ \leq \beta \leq 9.6^\circ$, assuming for example, a GSFC O_4 model for \hat{N} [Acuña and Ness, 1976]. We need to relate β to the phase of Jupiter's rotation at a given spacecraft observing time and position. Recognizing that to zeroth order

$$d\hat{N}/dt = \hat{\Omega} \times \hat{N} \quad (1)$$

where $\hat{\Omega}$ is Jupiter's angular velocity ($\hat{\Omega} = \Omega \hat{Z}$, for constant Ω), and integrating (1) gives



a) SHARP NOSE



b) BLUNT NOSE

Fig. 13. Meridian plane sketches of (a) a sharp-nosed obstacle (i.e., flattened approximately along the rotation axis) to solar wind flow whose front-side radius of curvature (r_c) is small compared to the solar wind stagnation distance (R_{SP}), representing a possibility for Jupiter's magnetosphere, and (b) a blunt-nosed obstacle whose r_c is comparable to R_{SP} , resembling the earth's case. In both cases the subsolar magnetosheath thickness $\Delta R = (R_{BS} - R_{SP})$ is expected to be much smaller for the sharp obstacle than for the blunt obstacle, where other considerations are assumed similar (e.g., the obstacle shape in the ecliptic plane view), then an estimate of $\Delta R/R_{SP}$ provides a semi-quantitative measure of the degree of front-side bluntness. (Figure provided by A. Dessler, private communication, 1980)

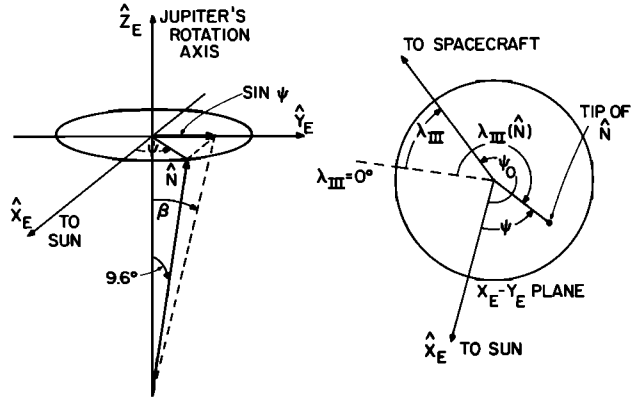


Fig. 14. A diagram (left) showing the motion of \hat{N} , the unit normal to the assumed rigidly co-rotating inner magnetosphere current disc, as a function of ψ and β , which are the X_E-Y_E (rotation plane) and Y_E-Z_E ('rocking plane') phase angles of \hat{N} , respectively. The angle ψ is defined in terms of the system III angles, λ 's, on the right. The subscript E on the coordinates refers to the Jupiter Equatorial System.

$$\tan \beta = \tan 9.6^\circ \sin \psi \quad (2)$$

where

$$\psi = \psi_0 + \lambda_{III} - \lambda_{III}(\hat{N}) \quad (3)$$

(from the X-Y and Y-Z projections of (1)), and where ψ , ψ_0 , λ_{III} and $\lambda_{III}(\hat{N})$ are defined in Figure 14, i.e., ψ is the angle from sun-line to X_E-Y_E projection of \hat{N} , ψ_0 is the angle from sun-line to spacecraft, λ_{III} is the system III longitude of spacecraft, and $\lambda_{III}(\hat{N})$ is the system III longitude of the X_E-Y_E projection of \hat{N} . For practical purposes the sun-line is assumed to be in the X_E-Y_E plane. Combining (2) and (3), and allowing for a phase change $\Delta > 0$ corresponding to the time for a feature to travel along (or near) the MP from a region near the stagnation point to the spacecraft, we obtain:

$$\beta = \tan^{-1} [\tan 9.6^\circ \sin(\text{Arg})] \quad (4)$$

where the argument of the sine function is

$$\text{Arg} \equiv \psi_0 + \lambda_{III} - \lambda_{III}(\hat{N}) - \Delta \quad (5)$$

We assume that the values of the phase angle β of the rocking magnetosphere determine the state of the MS field, i.e., whether the B_T component of the IMF (the most probable direction at Jupiter) remains steady or starts to turn 'northward' or 'southward' at or near the stagnation point ($X_E = 70 R_J$ nominally) as it is constrained to slide over the MP. To illustrate this, consider the Voyager 2 features where $\lambda_{III} \in 360^\circ$, i.e., the longitude where nineteen features shown in Figure 3 occurred. In particular we concentrate on δ -changes from north-to-south occurring clearly at 207 d, 0000 UT, and 2000 UT; 208 d, 1700 UT; and 214 d, 1100 UT. It is assumed that $\lambda_{III}(\hat{N}) = 202^\circ$, consistent with the longitude of the dipole portion of the GSFC O_4 model of the field of Jupiter [Acuña and Ness, 1976] and $\psi_0 = 226^\circ$. Hence, $\text{Arg} = 24^\circ - \Delta$. We assume that this switch

from north to south at the $X_E = 70 R_J$ plane occurs at $\beta \approx 0^\circ$. Figure 15 shows how a flattened magnetosphere rocking about the planet-sun line through the angle β may separate convected IMF field lines as they impact the MP and travel down the MS. When β is -9.6° (minimum) a westward IMF (i.e., $\lambda_{IMF} = 90^\circ$) will be draped southward in the MS, and when $\beta = 9.6^\circ$ (maximum) the IMF will be draped northward. For an eastward (i.e., $\lambda_{IMF} = 270^\circ$) and the same β 's the draping would be in the opposite sense to that associated with the westward IMF. $\beta = 0^\circ$ then is the 'separation-angle' between northward and southward MS fields depending on the sense of the IMF, expected to be predominantly the B_N component. Therefore, for $\beta = 0^\circ$, $Arg_\delta = -180^\circ n$ ($n = 0, 1, 2, \dots$), and $\Delta = 24^\circ + 180^\circ n$. From the work of Spreiter et al. [1968] we estimate an average MS plasma speed along the MP from the subsolar point to the Voyager 2 position (curvilinear distance of $\approx 300 R_J$) to be ≈ 290 km/s, where the solar wind speed was ≈ 400 km/s, obtained from Voyager 1. The convected plasma delay was then 20.5 hours. Converting Δ ($= 24^\circ + 180^\circ n$) to time units (using $9.925 \text{ hours}/360^\circ$) and comparing to 20.5 hours, gives $n = 4.0$ for purely convected features. However, the phasing of β is such that an odd n is required; this is easily seen if the Arg is allowed to change by 2-1/2 hours, for example, to maximum β . A lower n would imply that a wave propagation speed must be added to the convection speed of 290 km/s. Trying $n = 3$ shows that a propagation speed tailward of 90 km/s (total speed of 380 km/s) is required to yield $\beta = 0^\circ$ and proper phasing. For $n = 3$ we see that Jupiter rotated one and half times during the MS traversal from $X_E = 70 R_J$ to Voyager 2 (obviously if the effective MP region for the discrimination to north or south MS fields is closer to the spacecraft than $X_E = 70 R_J$, then a wave speed lower than 90 km/s would be sufficient; the wave speed will be discussed below). Assuming $n = 3$ to be a reasonable estimate, then about 2-1/2 hours after $\beta = 0^\circ$ (i.e., for $\lambda_{IMF} = 90^\circ$ now) $Arg = 270^\circ$ and $\beta = -9.6^\circ$. For this minimum β the IMF, which was known to be in the $\lambda_{IMF} \approx 90^\circ$ direction at this time from Voyager 1 measurements, would be draped southward in the MS, as Figure 15 indicates. Figure 3 demonstrates these predicted southward fields at times 207^d, 0230 UT and 2230 UT, 208^d, 1930 UT, and 214^d, 1330 UT, for example, all 2-1/2 hours after the times listed above for the north-to-south changes. Obviously, other large perturbations are seen in Figure 3 which compete with our model of the north-south changes. Some of these are probably due to the naturally occurring waves and discontinuities in the IMF, and possibly also to a magnetosphere rocking motion about the Y_E axis, which will be investigated in a future study.

Is a MS wave speed of < 90 km/s reasonable for the conditions present at that time? We examined the more prominent changes shown in Figure 11 to see if the $v_N - B_N$ correlations were Alfvénic. A necessary (but not sufficient) condition that a fluctuation must satisfy to be identified as an Alfvén wave [Alfvén and Falthammer, 1963; Belcher et al., 1969] is

$$\vec{b} = \pm(4\pi\rho)^{1/2} \vec{v} \quad (6)$$

where \vec{b} is the vector perturbation in the magnetic field, \vec{v} is the perturbation in the plasma velocity, and ρ is the plasma mass density. The N-component of (6) was examined to see if the derived ρ agreed with the observed density ρ_{obs} . For the several cases tested there was agreement to within 50%. Using the derived density and the average magnetic field magnitude across these B_N fluctuations one derives a characteristic Alfvén speed of 60 ± 15 km/s, which is in good agreement with the required value of < 90 km/s and consistent with our model. So the flowing plasma in the MS is probably being deviated approximately 'northward' and 'southward,' as viewed in the equator plane of Jupiter, primarily by the rocking motion of a flattened magnetosphere about the $X_E -$ axis. The field lines frozen to this plasma are constrained to lie in a plane parallel to the MP especially in the MS close to the MP. The net tailward speed of the plasma and field fluctuations, from several minutes to 10 hours, is apparently a combination of a convected component (≈ 290 km/s) and an apparent propagation component (≈ 70 km/s) for this period (solar wind speed of ≈ 400 km/s). The waves appear to consist of highly non-linear perturbations according to this preliminary analysis. The rocking motion of the magnetosphere is apparently directly responsible for generating these waves.

As Figures 9 and 10 show the direction of the IMF field at Jupiter is not constrained to low latitudes at all times; the spread in δ is, in fact, quite considerable. Spreiter et al. [1968] demonstrate how easy it is to obtain steeply in-

DAWN-SIDE DRAPING OF MAGNETOSHEATH FIELD

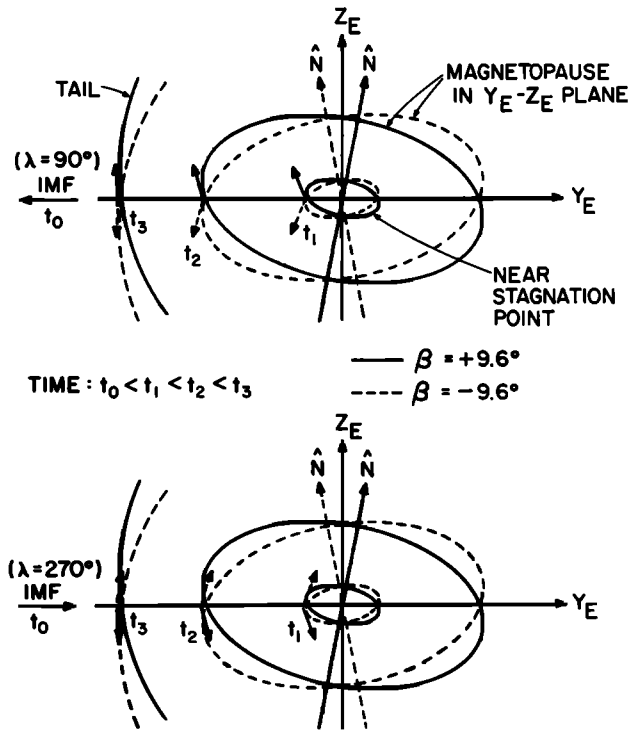


Fig. 15. A sketch representing the draping of magnetic field lines in Jupiter's MS, and a possible mechanism for producing the 5 and 10 hour field structures.

clined MS fields when there exists a significant IMF- B_N component for the earth's case, and indeed such a condition must contribute to our Jovian MS observations; see their Figures 25 and 26, for example. However, this is not the most probable state for the IMF at Jupiter, and when the IMF- B_N is significant it would probably play a less important role than the draping of the IMF- B_T component with respect to the 5 and 10 hour modulation.

We now address question (4), why are the north/south crossings occasionally synchronized with MP and BS crossings? Dessler and Vasyliunas [1979] suggest a range, in λ_{III} (1965) coordinates, in which the Voyager MP crossings should occur according to predictions from the magnetic anomaly model. The longitude $\lambda_{III} \approx 360^\circ$ was the longitude of greatest occurrence of Voyager 2 outbound MP crossing positions, as Figure 3 shows, and this longitude lies just outside the Dessler and Vasyliunas range. A 2-1/2 hour delay (or $\Delta\lambda_{III} = 90^\circ$) between the center of the predicted range and our $\lambda_{III} = 360^\circ$, explained possibly by magnetosphere propagation, would force agreement. We believe a more likely explanation for the quasi-periodic motion of the MP, and subsequently the BS, lies in understanding the motion and configuration of the magnetosphere current sheet, including especially the tail current sheet. If the motion of the tail current sheet has a direct influence on the tail MP motion along with solar wind changes, then it is obvious that tail MP crossings will be synchronized with β (through λ_{III}) for a fixed Δ , since ψ_0 and $\lambda_{III}(N)$ are essentially constant. Synchronization with β means synchronization with north/south crossings of the field in the MS as we argued above. Why the north/south changes are sometimes nearly phase locked with the boundary crossings is difficult to understand, but it could be a coincidence in which case it should disappear for a different trajectory (i.e., different ψ_0). This is suggested by a Voyager 1 and 2 comparison; Voyager 1 shows some synchronization but few boundary crossings at $\lambda_{III} = 360^\circ$.

In order to answer question (5) properly, concerning analogy with the earth's MS, would require a statistical study of that region. However, to show that steeply inclined fields do exist in the earth's MS Figure 16 is presented. It shows ≈ 31 hours of duskside MS field data from Imp 8. The average position of the spacecraft at this time in Cartesian GSE was $X = -16.4 R_E$, $Y = 30.1 R_E$, and $Z = 1.1 R_E$ (where R_E is the earth's radius). The figure does show similarities to the Jovian MS, especially the inbound MS: lower latitudes near the BS and large scale, and rapid, latitude variations as the MP is approached. However, to our knowledge there has been no report of 12 or 24 hour field structures in the earth's MS, although steeply inclined fields, i.e., 'north/south' orientations as shown in Figure 16 are well known (see Figures 5 and 8 in Fairfield [1976], for example). The occurrence probability of such steep north/south field inclinations in the earth's MS in the ecliptic plane, for example, is not known. We suggest that random samples of the earth's MS would not generally yield latitude histograms resembling those in Figure 9 for the early MS cases. The dramatic bimodal appearance of almost all of the

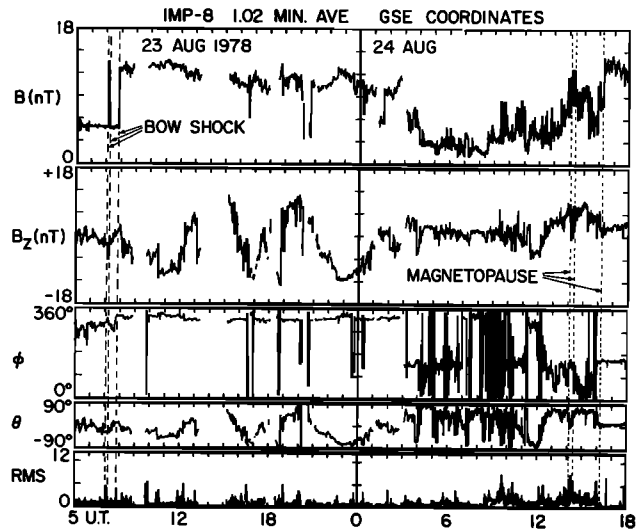


Fig. 16. An example of primarily MS magnetic field data (1.02-min averages) along the orbit of Imp 8 in geocentric solar ecliptic (GSE) coordinates. B is the field magnitude, ϕ is the longitude where $\phi = 0^\circ$ toward the sun, θ is the latitude, and B_z is the field component normal to the ecliptic plane. Note particularly the large north/south inclinations of the field becoming more pronounced as time progresses from BS to MP.

MS δ -histograms of Figure 9 and the presence of 5 or 10 hour quasi-periodic MS structures, especially in Voyager 2's case, argues fairly convincingly that the large scale features in Jupiter's MS are for the most part a uniquely Jovian characteristic and must be explained by forces of internal origin. An exception to this remark concerns the variation in the sense of the B_N - V_N correlation, positive or negative, which we now know depends simply on the direction of the ecliptic plane component of the impinging IMF; this component was predominantly aligned with \hat{t} during the outbound legs of both Voyager encounters (Figure 11 and accompanying text) with parallel or antiparallel sense depending on the sense of the MS correlation as previously discussed.

Summary of Findings

This section presents a brief summary of our observations and findings in three categories, starting with the most firmly established observations and ending with some preliminary interpretations.

Firm Observations or Results

1. There is an unusually high occurrence of nearly north or south fields in the outbound MS, especially in the vicinity of the MP.
2. The outbound MS fields and their variations tend to occur in a plane parallel to the local MP, according to reasonable large scale MP models.
3. An Alfvén wavelike correlation exists between variations in the plasma velocity and magnetic field in the outbound MS.
4. The 'north-south' field is also prevalent

in the inbound MS but usually only quite close to the MP and generally having a shorter time scale for its variation.

Less Firmly Established Results

1. Appearance of 5 or 10 hour quasi-periodicities appear in the outbound MS, especially in Voyager 2 data, which is more extensive.
2. Comparing Jupiter's and earth's MS's indicates obvious differences, in that no known 12 or 24 hour periodicities exist in the earth's case and north-south fields in the earth's MS are infrequent compared to Jupiter's case.
3. Occasionally (especially for Voyager 2), an apparent synchronization occurs between the large north-south MS field changes and some MP and BS boundary crossings.

Preliminary Interpretation

1. The occurrence of north-south fields and 5 or 10 periodicities is tentatively explained in

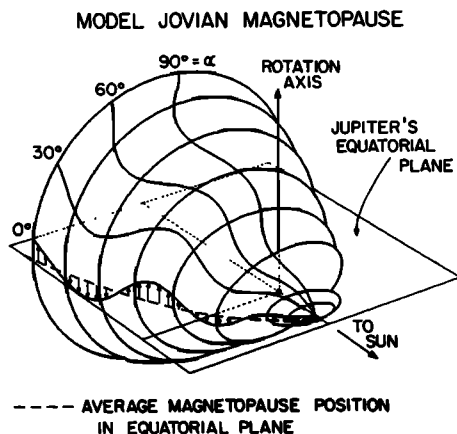


Fig. 17. A model of the dynamical magnetopause of Jupiter. It is assumed that near the vicinity of the nose of Jupiter's magnetosphere the intersection of the magnetopause surface with a plane perpendicular to the Jupiter-Sun line is an ellipse owing to an internal magnetospheric disc-like current sheet. The ratio of the semi-major and semi-minor axes is chosen such that it is equal to that given by Engel and Beard [1980] for the ellipse in the plane which contains the rotation axis. It is assumed that on the tailward side, far from the planet ($R \geq 250 R_J$), the tail cross-section is a circle. As the planet rotates, an ellipse near the nose oscillates about the Jupiter-Sun line. Information about the orientation of this ellipse propagates tailward at a speed which equals the sum of the Alfvén speed and the bulk speed in the magnetosheath near the magnetopause (see text). The dashed line is the model magnetopause derived from magnetopause crossings as discussed by Lepping et al. [1980]. Thus, the curve marked $\alpha = 0^\circ$ is the locus of the points on the semi-major-axes of a family of ellipses which oscillate about the Jupiter-Sun line. Similarly for the higher latitude α 's, that is, $\alpha = 90^\circ$ is the semiminor-axis locus of such points. The magnetopause surface is shown here as it would be seen by an observer 30° away from the Jupiter-Sun line in the equatorial plane and 30° above that plane.

terms of MS field line draping around a rocking magnetosphere whose period is synchronous with Jupiter's rotation period. See Figure 17 which shows a speculative sketch, with realistic dimensions, of Jupiter's dynamic MP with associated MS flow lines.

2. The magnetosphere is probably flattened, i.e., shorter in the north-south direction than in the east-west direction, or there is a bulge in the MP around the region of the equatorial plane giving the effect of a flattened magnetosphere.

The large current sheet that surrounds Jupiter and which is inclined with respect to Jupiter's equatorial plane is a distinguishing magnetospheric feature of great importance. The basic point that we have attempted to make is that the effects of this current sheet probably extend beyond the magnetosphere into the magnetosheath. The dynamical processes involved are not fully understood, but the kinematic effects alone can be significant in producing the magnetosheath phenomena that we have observed and described.

Acknowledgments. We wish to thank our Voyager magnetometer and plasma science colleagues, especially N. F. Ness and H. Bridge, the principal investigators, and J. Belcher and G. L. Siscoe for their many helpful remarks and assistance. We thank M. H. Acuña, K. W. Behannon and F. M. Neubauer for comments on the manuscript. We are grateful to the National Space Science Data Center at Goddard Space Flight Center for rapidly providing us with the Pioneer 10 magnetic field data of E. J. Smith and co-workers. We acknowledge useful discussions with A. J. Dessler, M. L. Kaiser, and J. E. P. Connerney. We thank our entire data processing team under W. Mish for their assistance with data analysis, handling and display, and for this work we thank specifically P. Alexander, P. Harrison, F. Ottens, A. Silver, M. Silverstein, and T. Vollmer.

References

- Acuña, M. H., and N. F. Ness, The main magnetic field of Jupiter, *J. Geophys. Res.*, **81**, 2917, 1976.
- Alfvén, H., and G.-G. Falthammar, *Cosmical Electrodynamics*, 2nd ed., Oxford at the Clarendon Press, London, 1963.
- Beard, D. B., and D. J. Jackson, The Jovian magnetic field and magnetosphere shape, *J. Geophys. Res.*, **81**, 3399, 1976.
- Behannon, K. W., Heliocentric distance dependence of the interplanetary magnetic field, *Rev. Geophys. Space Phys.*, **16**, 125, 1978.
- Behannon, K. W., M. H. Acuña, L. F. Burlaga, R. P. Lepping, N. F. Ness, and F. M. Neubauer, Magnetic field experiment for Voyagers 1 and 2, *Space Sci. Rev.*, **21**, 235, 1977.
- Behannon, K. W., L. F. Burlaga, and N. F. Ness, The Jovian magnetotail and its current sheet, *J. Geophys. Res.*, this issue.
- Belcher, J. W., L. Davis, Jr., and E. J. Smith, Large amplitude Alfvén waves in the interplanetary medium: Mariner 5, *J. Geophys. Res.*, **74**, 2302, 1969.
- Bridge, H. S., J. W. Belcher, R. J. Butler, A. J. Lazarus, A. M. Mavretic, J. D. Sullivan, G. L. Siscoe, and V. M. Vasyliunas, The plasma

- experiment on the 1977 Voyager mission, Space Sci. Rev., 21, 259, 1977.
- Bridge, H. S., J. W. Belcher, A. J. Lazarus, J. D. Sullivan, R. L. McNutt, F. Bagenal, J. D. Sudder, E. C. Sittler, G. L. Siscoe, V. M. Vasylunas, C. K. Goertz, C. M. Yeates, Plasma observations near Jupiter: Initial results from Voyager 1, Science, 204, 987, 1979a.
- Bridge, H. S., J. W. Belcher, A. J. Lazarus, J. D. Sullivan, F. Bagenal, R. L. McNutt, Jr., K. W. Ogilvie, J. D. Scudder, E. C. Sittler, V. M. Vasylunas, C. K. Goertz, Plasma observations near Jupiter: Initial results from Voyager 2, Science, 206, 972, 1979b.
- Carbary, J. F., Periodicities in the Jovian magnetosphere: Magnetodisc models after Voyager, Geophys. Res. Lett., 7, 29, 1980.
- Connerney, J. E. P., M. H. Acuña, and N. F. Ness, Modeling the Jovian current sheet and inner magnetosphere, J. Geophys. Res., this issue.
- Dessler, A. J., and V. M. Vasylunas, The magnetic anomaly model of the Jovian magnetosphere: predictions for Voyager, Geophys. Res. Lett., 6, 37, 1979.
- Engle, I. M., and D. B. Beard, Idealized Jovian magnetosphere shape and field, J. Geophys. Res., 85, 579, 1980.
- Fairfield, D. H., Average and unusual locations of the earth's magnetopause and bow shock, J. Geophys. Res., 76, 6700, 1971.
- Fairfield, D. H., Magnetic fields of the magnetosheath, Rev. Geophys. Space Phys., 14, 117, 1976.
- Goertz, C. K., Jupiter's magnetosphere: Particles and fields, Jupiter, edited by T. Gehrels, p. 32, University of Arizona Press, Tucson, 1976.
- Hill, T. W., A. J. Dessler, and F. C. Michel, Configuration of the Jovian magnetosphere, Geophys. Res. Lett., 1, 3, 1974.
- Intriligator, D. S., and J. M. Wolfe, Results of the plasma analyzer experiment on Pioneers 10 and 11, Jupiter, edited by T. Gehrels, p. 848, University of Arizona Press, Tucson, 1976.
- Kennel, C. F., and F. V. Coroniti, Jupiter's magnetosphere, Ann. Rev. Astron. Astrophys., 15, 389, 1977.
- Krasnov, N. F., Aerodynamics of Bodies of Revolution, edited by D. N. Morris, pp. 576-585, Elsevier, New York, 1970.
- Krimigis, S. M., T. P. Armstrong, W. I. Axford, C. O. Bostrom, C. Y. Fan, G. Gloeckler, L. J. Lanzerotti, E. P. Keath, R. D. Zwickl, J. F. Carbary, D. C. Hamilton, Hot plasma environment at Jupiter: Voyager 2 results, Science, 206, 977, 1979.
- Lepping, R. P. and K. W. Behannon, Magnetic field directional discontinuities, 1, Minimum variance errors, J. Geophys. Res., 85, 4695, 1980.
- Lepping, R. P., L. F. Burlaga, and L. W. Klein, Jupiter's magnetopause, bow shock and 10-hour modulated magnetosheath: Voyagers 1 and 2, Geophys. Res. Lett., 8, 99, 1981.
- Ness, N. F., M. H. Acuña, R. P. Lepping, L. F. Burlaga, K. W. Behannon, and F. M. Neubauer, Magnetic field studies at Jupiter by Voyager 1: Preliminary results, Science, 204, 982, 1979a.
- Ness, N. F., M. H. Acuña, R. P. Lepping, L. F. Burlaga, K. W. Behannon, and F. M. Neubauer, Magnetic field studies at Jupiter by Voyager 2: Preliminary results, Science, 206, 966, 1979b.
- Ness, N. F., M. H. Acuña, R. P. Lepping, K. W. Behannon, L. F. Burlaga, and F. M. Neubauer, Jupiter's magnetic tail, Nature, 280, 799, 1979c.
- Siscoe, G. L., N. U. Crooker, and J. W. Belcher, Sunward flow in Jupiter's magnetosheath, Geophys. Res. Lett., 7, 25, 1980.
- Smith, E. J., L. R. Davis, Jr., and D. E. Jones, Jupiter, edited by T. Gehrels, University of Arizona Press, Tucson, 1976.
- Sonnerup, B. U. O., and L. J. Cahill, Magnetopause structure and attitude from Explorer 12 observations, J. Geophys. Res., 72, 171, 1967.
- Spreiter, J. R., A. Y. Alksne, A. L. Summers, External aerodynamics of the magnetosphere, in Physics of Magnetosphere, edited by R. L. Carovillano, D. Reidel, Hingham, Mass., 1968.
- Vasylunas, V. M., Theoretical models of magnetic field line merging, 1, Rev. Geophys. Space Phys., 13, 303, 1975.

(Received June 18, 1980;
revised November 3, 1980;
accepted November 4, 1980.)